ELSEVIER

Journal of Nuclear Materials 244 (1997) 131–140

journal of nuclear materials

Modelling of fission gas release and gaseous swelling of light water reactor fuels

Toshiaki Kogai *

Toshiba Corporation, Shinsugita-machi 8, Isogo-ku, Yokohama-shi, Kanagawa-ken 235, Japan

Received 5 July 1996; accepted 27 November 1996

Abstract

Modelling to investigate the behavior of fission gas atoms of light water reactor fuels is elaborated. The model features the treatment of the grain boundary assumed to consist of two zones for solute gas atoms and intergranular bubbles. This, along with the athermal diffusion of fission gas atoms, enables the retention of gas during the base irradiation and the instantaneous release at temperature rise. The number density of intergranular bubbles varies upon interlinkage to express the saturation of the gaseous swelling after the gas release. Gas release at power reduction is dealt with considering the effective tensile stress acting on the grain boundary. The model is verified with four kinds of data from the irradiated fuels with known temperatures and confirmed to simulate fission gas release in a wide range of burnup, the time-dependency of gas release and porosity change in pellet, the decrease of gas release onset temperature with burnup, and the gas release at the power reduction.

1. Introduction

The behavior of fission gas atoms is an important discussion item respecting the light water reactor fuels, since they give rise to temperature increase and rod internal pressure buildup. Numerous models therefore have been developed to predict the amount of fission gas released into the free volume of the fuel rod. In the meantime, it is also important to grasp the behavior of fission gas bubbles precipitated in pellets when fuels are to be utilized to higher burnup, because a longer residential time in reactors brings about the decrease of as-fabricated gap and the bubble swelling leads to the intense mechanical interaction between pellet and cladding. Since bubble swelling is caused by fission gas atoms diffusing in pellets, the resulting interaction should be enhanced with time duration at high power (high temperature). Imamura et al. [1] pointed out that cladding deformation during ramp tests increased with time at high power. Actually, for the two fuel rods ramp-tested from 30 to 45 kW/m at the burnup of 48 GWd/tU, cladding permanent deformations recorded ca. 0.5% and ca. 1.0%, respectively, for 10 min and 240 min hold time cases. On the other hand, Ohara et al. [2] revealed that the cladding permanent deformations increased with burnup and decreased by the insertion of power dips from high power, referring to the ramp-tested fuel rods with burnup levels and ramp power histories as test parameters. Kogai and Iwano [3] analyzed those and their own results to show that these cladding deformations were effected by the creep of interacted cladding and the interaction was brought forth by the combination of the pellet–cladding differential thermal expansion and the pellet bubble swelling. Reduction of the cladding deformations by the power dips was attributed to the release of fission gas from the pellets leading to the reduction of swelling force. If one tries to elucidate the effects of fission gas atoms on high burnup fuel rod behavior, it is indispensable to properly model the fission gas bubbles.

Fission gas bubbles reside in grains as small intragranular bubbles and on grain boundaries as relatively large intergranular bubbles, and the latter contribute mainly to the volume increase of pellet. Prediction of the size and the number density of intergranular bubbles is hence important

* Tel.: +81-45 770 2032; fax: +81-45 770 2117; e-mail: kogai@rdef.iec.toshiba.co.jp.

PII S0022-3115(96)00731-3

as the basis of the calculation of swelling volume. Models to date, however, seem to be insufficient in this context. Some models assume the number density of intergranular bubbles to be constant throughout a fuel life [4–6]. This assumption obviously contradicts the fact that the bubbles decrease their numbers after interlinkage and may lead to the overestimation of bubble swelling, allowing overlapped bubbles. The model of Matthews and Wood [7] treats the change of the number density of intergranular bubbles to be a function of temperature, namely decreasing with the increase of temperature and vice versa. This treatment seems to be lacking in the consideration of time dependency of bubble growth. Tucker [8,9] presents elaborate models to describe the spacing of intergranular bubbles and the transfer of fission gas between grain faces and edges. These models are useful for mechanistic understanding of the behavior of intergranular bubble, but not necessarily applicable to producing numerical results.

This paper proposes a relatively simple but practical model to deal with the fission gas transfer in grain and grain boundary, the gas bubble swelling, and the stress dependent gas release. In the model, uniformly distributed intergranular bubbles grow and their number decreases after geometrical interlinkage point. The bubble size is correlated to its number density based on the laboratory data of irradiated UO_2 pellets [10,11]. The model, combined with Booth's equivalent sphere model [12] to deal with gas atom diffusion in matrix and the bubble growth model based on vacancy diffusion by Speight and Beeré [13], is capable of depicting the saturation behavior of bubble swelling, letting the volume swelling proportionate to r_{bl}^3 before interlinkage and to r_{bl} after interlinkage, r_{bl} being a bubble radius. It is widely known that an increase of rod internal pressure is often observed at the power reductions [2,3,14]. This implies that gas release from grain boundary to the free volume takes place when PCMI (pellet cladding mechanical interaction) is reduced. In the present model, the hydrostatic pressure in pellet is taken into account as the force acting on the grain boundary.

The verification of the model against the irradiation data revealed that the model could simulate the gas release and bubble swelling satisfactorily in a wide range of burnup up to 50 GWd/tU. If a considerable disagreement were to emerge in the future in much higher burnup fuels, that would present a good opportunity for developing new models, such as, intragranular bubble swelling model.

2. The model structure

Fig. 1 [15] shows a fracture surface of pellet which experienced high power at extended burnup. Grain boundaries are decorated with many bubbles, and interlinked pores are observed along the intersection of grain boundaries. This condition of pellet can make one envisage the following process for fission gas release.

Fission gas atoms generated in grain diffuse towards the grain boundaries through the repeated interaction with intragranular bubbles [16]. A part of the gas atoms which reach the vicinity of grain boundaries are swept out to the grain boundaries with grain growth. Although a part of the gas atoms which reach grain boundaries via these two processes are dissolved back to grain interior by irradiation [16], most of the gas atoms form intergranular bubbles and induce the volume increase of pellet. Intergranular bubbles grow with inflow of gas atoms and create passage for gas via interlinkage with adjacent bubbles. When gas is released through this passage and the release outweighs the supply of gas atoms, the pressure of bubbles decreases and bubbles cease to grow and shrink and are annihilated. The size of bubbles is determined by the balance of this supply of fission gas atoms from the grain and the release of the gas to the free volume. Here, this process is modelled as follows.

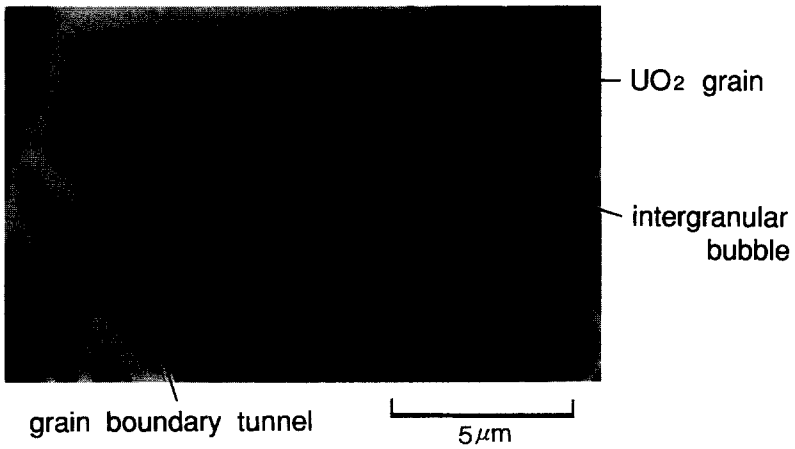

Fig. 1. A typical fracture surface of UO_2 pellet irradiated at high power at extended burnup [15].

The diffusion of fission gas atoms in grain is described by the radial concentration distribution in a simplified spherical grain. The sweeping of gas atoms is proportional to the grain growth rate and in-grain gas atom amount. The grain boundary consists of two zones, namely, the grain boundary surface, where fission gas atoms exist as solute atoms, and the intergranular bubble, where they exist as gas. Fission gas atoms diffusing to the grain boundary are allocated to the grain boundary surface and the intergranular bubble depending on the ratio of bubble coverage to total area of grain boundary, and the gas atoms on grain boundary surface diffuse to the intergranular bubbles along the concentration gradient. Intergranular bubbles are assumed to be spherical, and they grow or shrink depending on the difference between bubble pressure and hydrostatic stress imposed on them. The number density of intergranular bubbles is constant before the interlinkage, and then decreases with the growth of the bubbles after the geometrical interlinkage point.

The gas release from the grain boundaries to the fuel rod free volume takes place via a cylindrical thin tube. Assuming that gas flows in this tube from the high to low pressure end, i.e., from intergranular bubble to the free volume, we define the gas flow conductance of the tube. The conductance is taken as a function of both bubble coverage and stress working on the grain boundary, since gas release is accelerated with interlinkage of bubbles and suppressed by PCMI. Here, the stress imposed on the grain boundary is defined as a sum of pellet hydrostatic pressure (compressive) and gas bubble pressure (tensile). The idea of thin tube stems from the observation of gas release behavior of the fuel rod held at high power, when the pressure increase is suppressed and resembles the leak of gas through a pinhole [14].

3. Mathematical expressions of the model

Fission gas atoms move from grain interior to grain boundary and intergranular bubble, and from grain boundary to intergranular bubble, and then from intergranular bubble to the free volume in succession. Under this assumption, the conservation of the gas amount in grain boundary and intergranular bubble is written as

$$\dot{m}_{gb} = (1 - F_c) J_1 - J_2, \tag{1}$$

$$\dot{m}_{bl} = F_c J_1 + J_2 - J_3. \tag{2}$$

Here, m_{gb} is the gas amount in grain boundary (m^{-3}), m_{bl} is the gas amount in intergranular bubble (m^{-3}), J_1 is the gas flow from grain interior to the grain boundary (m^{-3} s^{-1}), J_2 is the gas flow from grain boundary to intergranular bubble (m^{-3} s^{-1}), J_3 is the gas flow from intergranular bubble to the free volume (m^{-3} s^{-1}), and F_c is the bubble coverage of grain boundary (-).

The bubble coverage of grain boundary F_c is described as follows by using the gas bubble radius r_{bl} (m) and bubble spacing s (m),

$$F_c = \frac{\pi r_{bl}^2}{s^2}. \tag{3}$$

The bubble spacing s is correlated to the number density of intergranular bubble N_{bl} (m^{-2}) as

$$N_{bl} s^2 = 1. \tag{4}$$

The gas flow from grain interior to the grain boundary J_1 is written as

$$J_1 = J_D + \alpha m_{gr} \frac{\dot{r}_{gr}}{r_{gr}}. \tag{5}$$

Here, J_D is the amount of the gas diffusing directly from grain to the grain boundary (m^{-3} s^{-1}), α is the parameter to define the gas sweeping efficiency by grain growth (-), m_{gr} is the gas amount in grain (m^{-3}), and r_{gr} is the grain radius (m).

J_D is expressed by

$$J_D = G - \dot{m}_{gr}, \tag{6}$$

with the generation rate of fission gas atoms G (m^{-3} s^{-1}). The gas amount in grain m_{gr} is given averaging by volume the gas atom concentration c_{gr} in a hypothetical spherical grain,

$$\dot{m}_{gr} = \frac{3}{r_{gr}^3} \int_0^{r_{gr}} c_{gr} r^2 \, dr. \tag{7}$$

The gas atom concentration c_{gr} is calculated by applying the finite element method for spatial discretization to the one-dimensional diffusion equation in the spherical system following the two-zone scheme by Matthews and Wood [17].

The gas flow from grain boundary to the intergranular bubble J_2 is written as

$$J_2 = 4\pi N_{bl} r_{bl} m_{gb} D_{gb} / s, \tag{8}$$

with the diffusion coefficient of gas atom on the grain boundary D_{gb} (m^2 s^{-1}). This equation is derived by assuming that the gas atom concentration in the gas bubble is zero and by converting into the amount per unit volume of grain the diffusing amount of gas to the intergranular bubble.

The gas flow from intergranular bubble to the free volume J_3 is defined as

$$J_3 = \frac{V_c N_{bl} P_{bl}^2}{\eta k T r_{gr}}, \tag{9}$$

by considering the hypothetical thin tube between the intergranular bubble and the free volume. In accordance with the vacuum theory, the gas flow amount S (m^3 Pa/s) between the two ends of different pressure, P_1 and P_2, is written as $S = \pi a^4 (P_1 + P_2)(P_1 - P_2)/16\eta^2 L$, with a,

the tube radius, and L, the tube length. Eq. (9) is deduced based on this equation, neglecting the pressure in the free volume since it is usually far smaller than the one in the intergranular bubble, and converting the unit of S to the one for the number of gas atoms per unit grain. Here, V_c is the volume of the tube (m^3), P_{bl} is the gas pressure of the intergranular bubble (Pa), η is the gas viscosity ($\mu P = 10^{-7}$ N s/m^2), k is the Boltzmann constant ($= 1.3807 \times 10^{-23}$ J/K), and T is the absolute temperature (K).

The gas viscosity η [18] is

$$\eta = 26.69 \frac{\sqrt{MT}}{\zeta^2}. \tag{10}$$

Here, M is the molecular weight of gas atom (-), and ζ is the hard-sphere diameter (m).

The volume of the tube V_c determines the conductance of the gas in the thin tube. The gas flow is assumed to increase by the shortening of the tube and/or thickening of the tube, and V_c is described as the product of the two monotonically increasing functions of bubble coverage of grain boundary F_c and the effective tensile stress acting on the grain boundary σ_e, respectively.

$$V_c = V_c^{\circ} f(F_c) g(\sigma_e). \tag{11}$$

Here, V_c° (m^3) is equal to $3\pi a^4/32L$. A σ_e is defined as the sum of the hydrostatic pressure imposed on pellet σ (compressive), and the bubble pressure P_{bl} (tensile),

$$\sigma_e = \frac{\sigma s^2 + \pi r_{bl}^2 P_{bl}}{s^2 - \pi r_{bl}^2} = \frac{\sigma + F_c P_{bl}}{1 - F_c}. \tag{12}$$

The growth of a grain boundary bubble is written as follows, based on the vacancy diffusion induced by the pressure difference inside and outside of the bubble [7].

$$\dot{r}_{bl} = \frac{s^2 \delta_b D_{gb}^v \Omega}{4 r_{bl}^2 kT} (P_{bl} - P_h - 2\gamma \sin\theta / r_{bl}) k_f^2. \tag{13}$$

Here, δ_b is the grain boundary thickness (m), D_{gb}^v is the vacancy diffusion coefficient on grain boundary (m^2 s^{-1}), Ω is the atomic volume (m^3), P_h is the hydrostatic pressure imposed on pellet (Pa), γ is the surface tension of bubble on the grain boundary (N/m), and θ is the dihedral angle between the bubble and grain boundary surface (°).

The gas bubble pressure P_{bl} is calculated from the number of gas atoms per bubble $2m_{bl} r_{gr}/3N_{bl}$ as

$$P_{bl} = \frac{r_{gr} m_{bl} kT}{2\pi N_{bl} r_{bl}^3}. \tag{14}$$

A k_f^2 is the sink strength of the bubble given by the following equation [7],

$$k_f^2 = \frac{8(1 - r_{bl}^2/s^2)}{s^2 \left[(r_{bl}^2/s^2 - 1)(3 - r_{bl}^2/s^2) + 4\ln(s/r_{bl}) \right]}. \tag{15}$$

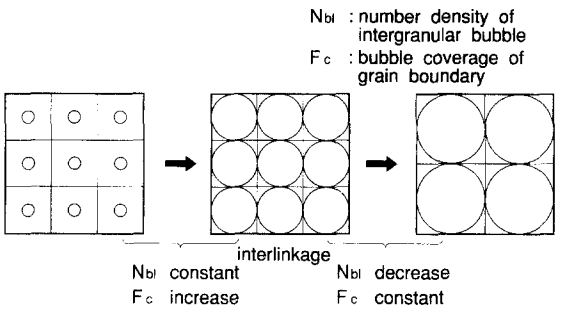

Fig. 2. Schematic diagram to illustrate the change of the number density of the intergranular bubble with its growth.

Kashibe and Une [10] propose the correlation between the bubble size and its number density based on their annealing test results of irradiated UO_2 fuels and the PIE data of ramp-tested fuels by Walker et al. [11]. The correlation suggests that the geometrical interlinkage condition $4N_{bl} r_{bl}^2 = 1$ for the uniformly arranged gas bubbles may apply approximately to the gas bubbles once interlinked. Accordingly, the present model expresses the correlation between the number density of the bubble N_{bl} and the bubble radius r_{bl} as follows.

$$N_{bl} = \begin{cases} N_{bl}^{\circ} & (r_{bl} < r_{bl}^{\circ}), \\ 1/4r_{bl}^2 & (r_{bl} \geq r_{bl}^{\circ}). \end{cases} \tag{16}$$

Here, N_{bl}° is the initial number density of the bubble. An r_{bl}° is derived from the interlinkage condition $F_c = \pi/4$ as $r_{bl}^{\circ} = 1/2\sqrt{N_{bl}^{\circ}}$: that is, the number density of the bubble is constant before interlinkage and bubble coverage increases with the growth of the bubble, while the bubble coverage becomes constant after interlinkage and the number density of the bubble decreases with the growth of the bubble. This process is illustrated in Fig. 2.

The pellet swelling due to the intergranular bubbles is written as

$$\Delta V/V = \frac{2\pi N_{bl} r_{bl}^3}{r_{gr}}, \tag{17}$$

using the number density of the bubble N_{bl}, bubble radius r_{bl} and grain radius r_{gr}. Based on the Eq. (16), the bubble swelling is proportional to the power of three of bubble radius r_{bl} before the interlinkage, but to the power of one after the interlinkage. This treatment may describe the saturation tendency of the bubble swelling after the significant gas release.

4. The applicability of the model

In order to obtain fission gas release and gaseous swelling by this model, Eqs. (1), (2) and (13) in the previous section and the diffusion equations in grain are

solved simultaneously. Here, a set of these equations, which is discretized for time by the backward Euler method, is linearized by the Newton–Raphson method for solution through iterative calculations. The calculation is carried out by dividing the pellet into ten equal volume rings.

The inputs to this model are time increment, fission density, fuel temperature and hydrostatic pressure in pellet. Since the uncertainty in fuel temperature makes model verification difficult, irradiation data, for which fuel temperature is measured directly by certain methods, are selected.

Table 1 lists the names of selected fuel specimens and fuel rods from four irradiation tests. The irradiation test A [19] examines the fission gas release behavior in the power rise test (called bump test) at the test reactor. The experimental details are shown in Ref. [19]. The test B [20] executes a steady-state irradiation at fairly high power at the test reactor by installing a fuel centerline thermocouple and a rod internal pressure sensor of bellows type at the fabrication of the rods. The test C [21] is aiming to irradiate wafered pellet specimen at the isothermal condition and investigate the fission gas release behavior based on the amount of retained gas in pellet after irradiation. The test D [22] examines the release behavior of rare gas, ^{85}Kr, by annealing the base-irradiated light water fuels in commercial reactors. The pellet hydrostatic pressure, believed to have existed during the bump tests for fuel rods of the test A, is calculated based on the cladding deformation data and the interactive force between pellets and cladding by assuming that the cause of deformation is the creep of cladding. Hydrostatic pressures in the other tests are considered to be virtually zero.

The materials data used in the calculations are given in Table 2. As well as the aforementioned fuel temperature, the in-grain diffusion coefficient of gas atoms affects the fission gas release. Table 3 compares the reported in-grain diffusion coefficients of gas atoms for UO_2. These are roughly categorized into three groups: the measurements by implanting fission gas atoms into UO_2 grain followed by annealing tests [23–26], the measurements in situ using gas-sweep rig [27–29], and the measurements of gas bubble growth rate or gas atom release rate by heating up UO_2 base-irradiated in commercial reactors [22,30,31]. Gas atoms are considered to be trapped by intragranular bubbles and then dissolved into the matrix under irradiation en route to the grain boundaries. The first group is supposed to represent the diffusion coefficient of fission gas atoms essentially in the absence of trapping by intragranular bubbles because of light irradiation. On the other hand, the diffusion coefficients of the last group are based on the specimens base-irradiated in commercial reactors and affected by the trapping by intragranular bubbles. The resolution of gas atoms is hardly expected because the tests are implemented under no irradiation and the measured effec-

Table 1
Verification database of fuel specimens with measured temperature

Test name	Test description	Specimen ID	Burnup (GWd/tU)	Remarks
A. The third Risø Project [19]	Short-length fuel rods, base-irradiated at commercial BWR and PWR, were refabricated with a thermocouple and a pressure gauge, and bump-tested (moderate power ramp rate and hold at the terminal power).	GE2	44	Pellet hydrostatic pressures were estimated based on the cladding deformations, as 50, 6, 17, 27, 27, 23 and 10 (MPa), respectively.
		GE4	23	
		GE6	43	
		AN3	42	
		AN4	42	
		AN10	42	
		II3	15	
B. The Halden irradiation test (IFA-501) [20]	Fuel rods with a thermocouple and a pressure gauge were irradiated at fairly high power.	A1	20	Pellet hydrostatic pressures were virtually zero.
		A2	25	
C. The isothermal irradiation test [21]	Disk pellets were irradiated at high neutron flux isothermally. Pellets were crashed and FGR was measured at various burnup levels.	Z1	100	Irradiation temperatures were 1250, 1500, 1750 and 2000 K, respectively.
		Z2	100	
		Z3	100	
		Z4	100	
D. The annealing test of irradiated pellets [22]	Small specimens were taken from mid-pellet position of base-irradiated BWR fuels. The specimens were annealed and ^{85}Kr was measured continuously.	U06	6	Held at 1800°C for 5 h.
		U16	16	ibid.
		U23	23	ibid.
		U28	28	ibid.
		U16S	16	Step-wise temperature increase.
		U28S	28	ibid.

Table 2
Data used in calculations

Surface tension of bubble γ	1 J/m^2
Dihedral angle θ	50°
Atomic volume Ω	4.09×10^{-29} m^3
Grain boundary thickness δ_b	5×10^{-10} m
Gas atom diffusion coefficient in grain D_{gr}	$D_a + D_b + D_c$ m^2/s
	$D_a = D_a^\circ \exp(-70000/RT)$
	$D_a^\circ = 7.6 \times 10^{-10} + 6.84 \times 10^{-9} B_u/40$
	B_u: GWd/t (40 is an upper limit)
	R: 1.987 cal/(mol · K)
	$D_b = s^2 j_v V$
	$s = \Omega^{1/3} = 3.4454 \times 10^{-10}$ m
	$j_v = 10^{13} \exp(-55200/RT)$ s^{-1}
	$V = (\alpha_s^2 + ZV_0)/2Z[(1 + 4K'Z/(j_v(\alpha_s s^2 + ZV_0)^2))^{1/2} - 1]$
	$\alpha_s = 10^{15}$ m^{-2}
	$Z = 100$
	$V_0 = \exp(-55200/RT)$
	$K' = 2 \times 10^{-4}$ s^{-1}
	$D_c = 2 \times 10^{-40} \dot{f}$, $\dot{f}$: fissions/(m^3 · s)
	for test D, $D_a = 6.4 \times 10^{-5} \exp(-132000/RT)$ [22]
	ibid for D_b, D_c
Gas atom diffusion coefficient in grain boundary D_{gb}	$6.9 \times 10^{-4} \exp(-77000/RT)$ m^2/s [a]
Vacancy diffusion coefficient in grain boundary D_{gb}^v	the same as D_{gb}
Grain growth rate $\dot{r}_{gr}$	$(5.922 \times 10^{16}/r_{gr}^3) \exp(-142000/RT)$ μm/s [34]
Gas sweep efficiency parameter α	10^{-3}
Initial number density of intergranular bubble N_{bl}°	10^{12} n/m^2
Molecular weight of gas M	131
Hard-sphere diameter ζ	4.047×10^{-10} m
Volume of the thin tube V_c	$V_c^\circ f(F_c) g(\sigma_c)$
	$f(F_c) = 1 - \exp[-(F_c/F_c^\circ)^n]$
	$g(\sigma_c) = 1 - \exp[-(\sigma_c/\sigma_c^\circ)^n]$
	$V_c^\circ = 10^{-12}$ μm^3, $n = 10$, $F_c^\circ = 0.78$, $\sigma_c^\circ = 10$ MPa

[a] A slight modification applied to Reynolds and Burton [33].

tive diffusion coefficients are supposed to be relatively small. Between these two groups exists the second group, which is believed to represent the diffusion coefficients of fission gas atoms under the conditions where the trapping and resolution occur at the same time. Fig. 3 depicts the diffusion coefficients referred to in Table 3. The present model incorporates the diffusion coefficient by Turnbull et al. [27], which belongs to the second group. The proces-

Table 3
Comparison of in-grain diffusion coefficients of fission gas atoms in UO_2

Author	Method	Atmosphere	Temperature (°C)	D_{gr} (m^2/s)
Miekeley and Felix [23]	annealing of lightly irradiated specimens	O/U ~ 2.0	950–1700	4×10^{-21}–6×10^{-15}
Matzke [24]	Xe isotope injection and annealing	O/U ~ 2.0	1000–1800	1×10^{-20}–1×10^{-15}
Matzke [25]	tracer diffusion	—	< 1000	$D^* = A\dot{F}$
Carter et al. [26]	Xe atom recoil injection and annealing	O/U ~ 2.0	1065–1300	3×10^{-19}–1×10^{-16}
Turnbull et al. [27]	measurement in situ with gas sweep rig	reduction	225–1400	1×10^{-21}–5×10^{-19}
Hirai et al. [28]	measurement in situ with gas sweep rig	Mo–MoO_2 equilibrium · reduction	300–1400	2×10^{-21}–1×10^{-18}
Findlay [29]	measurement in situ with gas sweep rig	O/U ~ 2.0	1000–2000	5×10^{-22}–1×10^{-16}
Cornell [30]	annealing of low burnup fuel	O/U ~ 2.0	1300–1500	5×10^{-21}–1×10^{-19}
Une and Kashibe [22]	annealing of high burnup fuel	reduction	1500–1800	1×10^{-21}–1×10^{-18}
Baker and Killeen [31]	annealing of high burnup fuel	oxidation · reduction	1000–1750	2×10^{-20}–2×10^{-17}

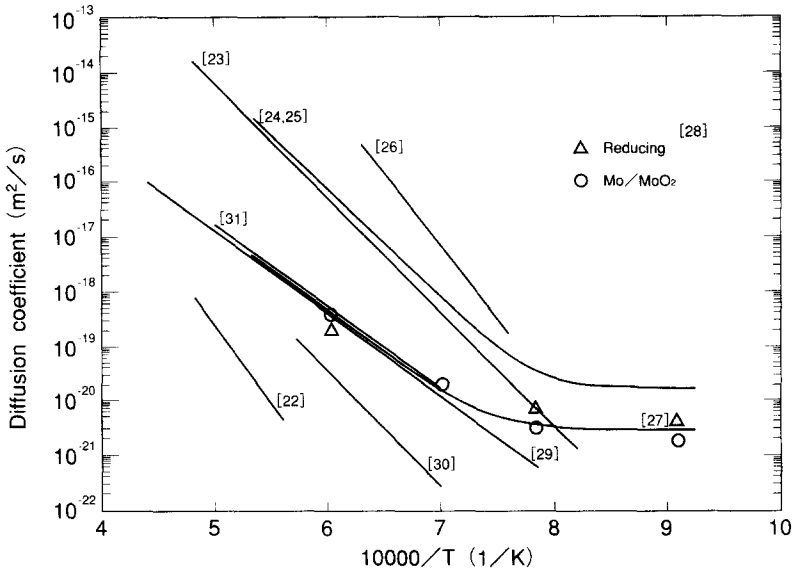

Fig. 3. In-grain gas atom diffusion coefficients of UO_2.

sion of irradiation, or burnup extension, increases radiation defects in pellets and produces subgrain boundaries [32], which might accelerate the diffusion coefficients. It turned out in the course of the verification of the model that the burnup dependency of diffusion coefficient is indispensable to explain the gas release data scattering in a wide range of burnup. In the model, the pre-exponential factor of the first 'intrinsic' diffusion term by Turnbull et al. [27] is increased continuously up to 40 GWd/tU to fit all the included data. The reason why the upper limit is set is attributed to the observation by Une et al. [32] that the accumulation of the radiation defects seems to be saturated around this burnup level.

Few reports are available for the grain boundary diffusion coefficients. Reynolds and Burton [33] propose a grain boundary diffusion coefficient of U^{4+} ion based on the results of the sintering test and the creep test of UO_2. Here, their equation is used with a slight modification as the grain boundary diffusion coefficient for gas atom and vacancy. The volume of the thin tube is expressed as the product of two sigmoidal curves as for the bubble coverage of grain boundary F_c and the effective tensile stress acting on the grain boundary σ_e. The initiation of fission gas release often resembles this type of curve. Fig. 4 compares the results of fission gas release calculated by the model and measured. The results agree within the relative error of about 30%. This is a reasonable agreement considering an intricate behavior of fission gas.

Fig. 5(a) shows the radial distribution of the residual xenon atoms measured by EPMA in fuel pellets after the bump tests with the bump terminal level of ca. 40 kW/m at 42 GWd/tU. The figure contains the results of three different non-refabricated fuel specimens (not listed in Table 1). The fuel temperature at the bump terminal level is estimated to be about 1600°C at the pellet center. The hold time in the bump tests was changed to ascertain the effects of time duration on the gas release, namely, to 4, 42 and 63 h, as shown in the figure. It is clear that the gas released area extends deeply in the radial direction when the hold time becomes longer at the bump terminal level. This indicates that the gas atom diffusion in grain and grain boundary proceeds with time. Fission gas atoms are exhausted up to in the region which has relative radius of 0.6 in fuel after 42–62 h. On the other hand, Fig. 5(b) and (c) show the calculation results of the residual gas atom fraction and the gaseous swelling when fuel pellet is steadily irradiated to 30 GWd/tU at fuel centerline temperature of 800°C, and then held at that of 1800°C for 1, 10 and 100 h, respectively. It is consistent with the experi-

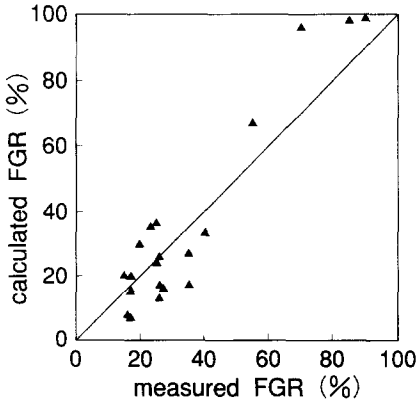

Fig. 4. Comparison of measured and calculated fission gas release.

mental findings that the gas release area widens toward the pellet peripheral region with time. Fig. 5(c) clarifies that the radial location giving the maximum gaseous swelling shifts to the periphery of the pellet. This is ascribed to the shrinkage of intergranular bubbles after the gas release.

In current light water reactor fuels for BWR and/or PWR, no significant amount of fission gas release has been observed during the base irradiation, since operating power is suppressed to a moderate level. Once transient phenomenon takes place, however, a considerable amount of fission gas is released from the fuel element at lower power for higher burnup fuels [35]. Given the considerably high in-grain diffusion coefficient of gas atoms of 1×10^{-17} m^2/s (1300°C), fission gas release to the grain boundary in 60 s is less than 1%. This implies that gas atoms may be accumulated on the grain boundary or in its vicinity prior to the power transients. The present model describes this gas atom accumulation by the athermal diffusion term (the third term) of the in-grain diffusion coefficient [27] and the function of grain boundary as a reservoir for gas atoms. Consequently, the gas atoms reaching the grain boundaries reside as solute atoms and are ready to be released to the free volume via growth and interlinkage of bubbles on the temperature rise. Fig. 6(a) shows the simulation of the fission gas release when temperatures of test specimens are raised step-wise as indicated by broken lines from 1000 to 2000°C with the step of 100°C at burnup of 5, 10, 20 and 30 GWd/tU. The pellet temperature during the base irradiation was kept low enough to suppress temperature-dependent gas diffusion. The figure shows that the gas release occurs from the lower temperature to a larger extent, if burnup proceeds. Fig. 6(b) shows the simulation of the fission gas release observed in the annealing tests of the pre-irradiated UO_2

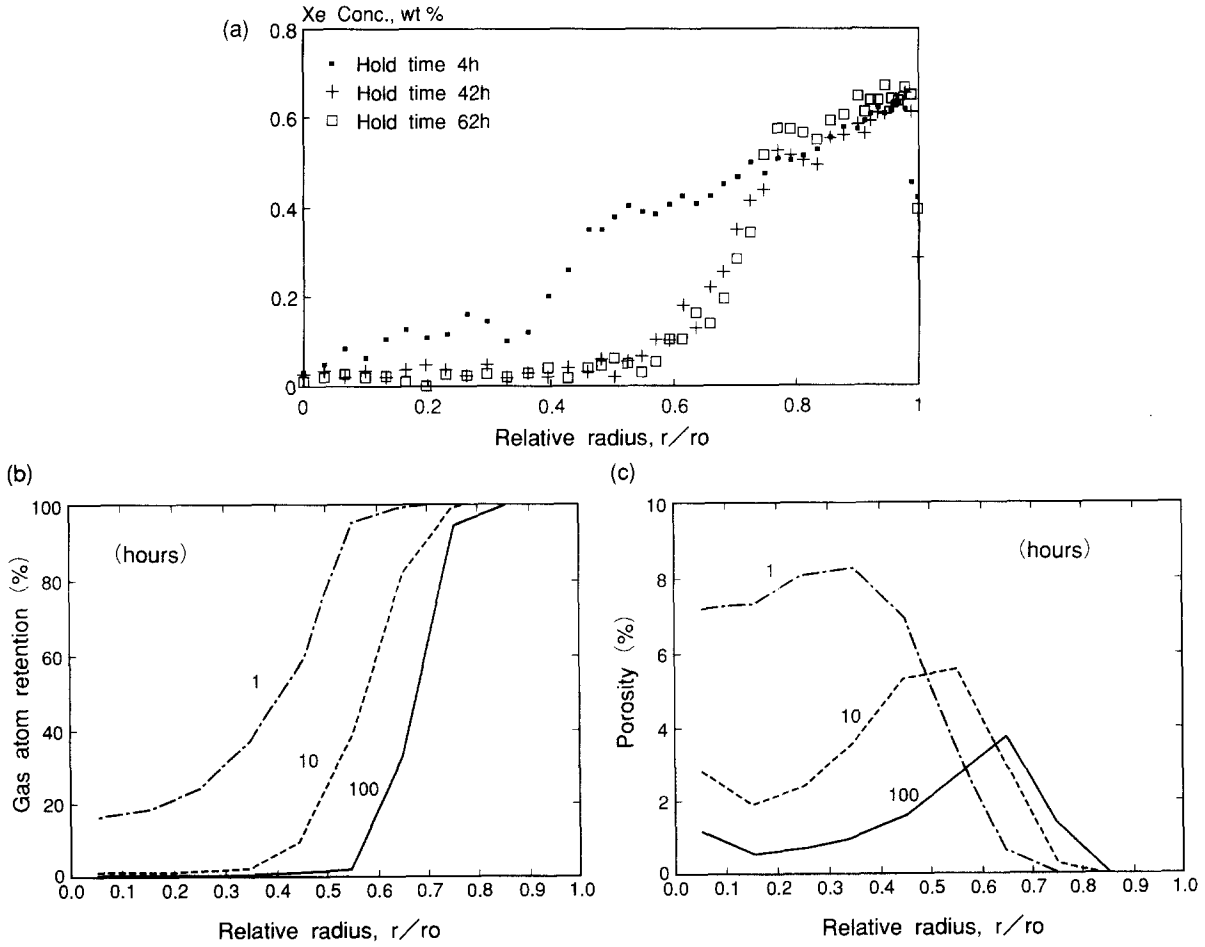

Fig. 5. (a) A retention profile of xenon atoms measured by EPMA after the bump tests of the ANF fuels to show the effect of hold time on fission gas release [19] (fuels are bump-tested at ca. 40 kW/m and estimated fuel centerline temperature is ca. 1600°C for all three specimens, which differ in the hold time duration). (b) Model prediction of the radial retention profile of xenon atom to show the effect of hold time (the release area extends more deeply into the fuel periphery with time). (c) Predicted change of porosity with time to show that the maximum porosity area moves toward the fuel periphery because of the shrinkage of the intergranular bubbles at the pellet center.

fuels [22]. The burnup after the base-irradiation is 16 and 28 GWd/tU, and a substantial burst release of gas is observed at 1600 and 1500°C, respectively, with a small additional gas release found after 1000°C. The calculation reproduces the release commencing temperature quite well. The release at the low temperature in the experiment may be attributable to the microcracks of pellet specimens during the preparation.

Fig. 7(a) and (b) compare the calculation and the measurement, for the specimen GE2 of the test A, of the fission gas release behavior during the bump test and the distribution of the residual fission gas atoms and the porosity in pellet after the bump test, respectively. A noteworthy phenomenon in the gas release behavior in Fig. 7(a) is the gas release of more than 10% at the single power reduction during the bump test. This gas release is considered to be due to the removal of the hydrostatic stress imposed on the pellets. The tested fuel cladding has a permanent deformation of 0.3% during the bump test,

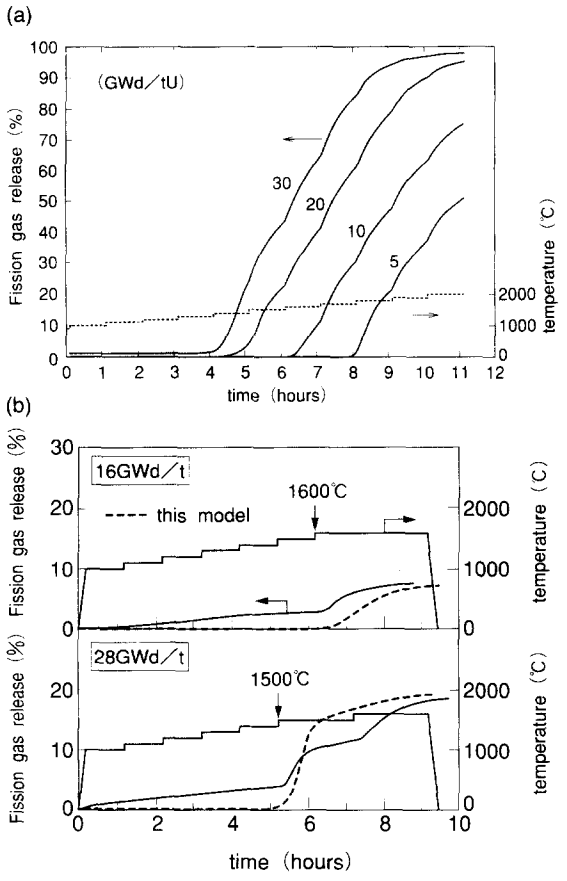

Fig. 6. (a) Model prediction of fission gas release at a temperature rise after the various burnup levels which indicates that gas release begins at the lower temperature with burnup. (b) Simulation of the onset temperature of fission gas release at annealing tests [22].

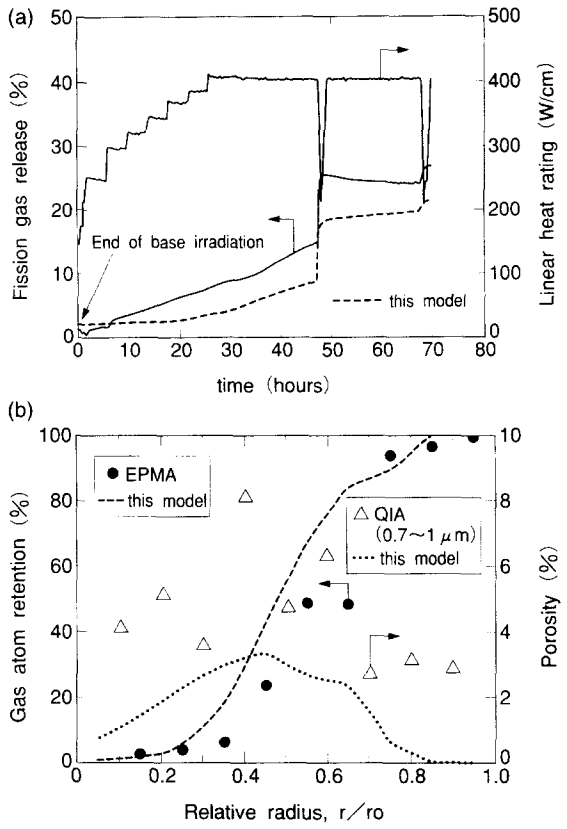

Fig. 7. (a) Simulation of the fission gas release behavior at the bump test of rod GE2 [19] in which the instantaneous gas release at the power reduction is characteristic. (b) Simulation of the gas retention and porosity in pellet after the bump test of rod GE2 [19] (calculated porosity includes only the one by intergranular bubbles).

which reveals that pellet and cladding are in hard mechanical interaction at the high power hold of the bump test. It is found that the model can simulate this gas release by reducing the pellet hydrostatic stress to zero at the power reduction. Fig. 7(b) compares the EPMA-measured gas atom retention profile with the calculated gas atom concentration in grain. The decrease of the gas atom concentration at the pellet relative radius of 0.6–0.7 is well simulated by the model. The porosity profile is also compared in the figure. The calculated porosity represents just a contribution of intergranular bubbles. It increases toward the mid-pellet in both the measurement and the calculation, rather than at the pellet center. This is interpreted as indicating that the shrinkage of the gas bubbles proceeds after the gas release because of the long hold time at high power (about 40 h). Although there is some discrepancy between measured and calculated porosities, an additional consideration of the change of as-fabricated porosity and the generation of 'rim' porosity would bring the model calculation up closer to the measured values.

5. Conclusions

Modelling has been tried to clarify the behavior of fission gas atoms at high burnup. The model features the treatment of the grain boundary, which is assumed to consist of two zones, for solute atoms and gas (intergranular bubble). This, along with the athermal diffusion term of fission gas atoms in grain, enables the retention of gas in pellet during the base irradiation and instantaneous release at the following temperature rise. Gaseous swelling seems to be saturated after the significant gas release, and is modelled by changing the number density of intergranular bubbles upon interlinkage. The gas release at power reduction, which is ascribed to the change of the stress state in pellet, is dealt with considering the effective tensile stress acting on the grain boundary.

This model has been verified with four kinds of data from irradiated fuels, for which temperatures are directly measured. The achievements are that (1) fission gas release is consistently predicted in a wide range of burnup, (2) the time-dependency of gas release and porosity in pellet is expressed, (3) the decrease of gas release onset temperature with burnup is well simulated, and (4) the gas release at the power reduction is reproduced with the retained fission gas in pellet in good agreement with the measurement.

It is concluded that this relatively simple model is able to simulate the fission gas release and gaseous swelling of light water reactor fuels at high burnup.

Acknowledgements

The author is grateful to Masao Ishida of Nippon Nuclear Fuel Development Co., Ltd. for his interest and valuable comments regarding this work.

References

[1] M. Imamura, K. Une, K. Isoda, T. Ikeda and T. Yamanaka, Preprint of 1993 Annual Mtg. of At. Energy Soc. Jpn. K38 (1993) (in Japanese).
[2] H. Ohara, T. Nomata, M. Irube, S. Iwata and M. Futakuchi, 1994 Int. Topical Meeting on Light Water Reactor Fuel Performance, West Palm Beach, FL, April 17–21 (1994) p. 674.
[3] T. Kogai and Y. Iwano, J. Nucl. Sci. Technol. 27(11) (1990) 1017.
[4] M.J.F. Notley and I.J. Hastings, Nucl. Eng. Des. 56 (1980) 163.
[5] K. Ito, R. Iwasaki and Y. Iwano, J. Nucl. Sci. Technol. 22(2) (1985) 129.
[6] M. Tayal, L.D. MacDonald, E. Kohn and W.P. Dovigo, Nucl. Technol. 85 (1989) 300.
[7] J.R. Matthews and M.H. Wood, J. Nucl. Mater. 91 (1980) 241.
[8] M.O. Tucker, J. Nucl. Mater. 74 (1978) 34.
[9] M.O. Tucker, J. Nucl. Mater. 75 (1978) 282.
[10] S. Kashibe and K. Une, J. Nucl. Sci. Technol. 28(12) (1991) 1090.
[11] C.T. Walker, P. Knappik and M. Mogensen, J. Nucl. Mater. 160 (1988) 10.
[12] A.H. Booth, Atomic Energy of Canada Limited Chalk River Report, CRDC-721 (1957).
[13] M.V. Speight and W. Beeré, Met. Sci. 9 (1975) 190.
[14] T. Kogai, K. Ito and Y. Iwano, J. Nucl. Mater. 158 (1988) 64.
[15] P. Knappik and C.T. Walker, Risø-TFGP-R24 (1986).
[16] M.V. Speight, Nucl. Sci. Eng. 37 (1969) 80.
[17] J.R. Matthews and M.H. Wood, Nucl. Eng. Des. 56 (1980) 439.
[18] R.C. Reid, J.M. Prausnitz and T.K. Sherwood, The Properties of Gases and Liquids, 3rd Ed. (McGraw-Hill, New York, 1977).
[19] C. Bagger, M. Mogensen and C.T. Walker, J. Nucl. Mater. 211 (1994) 11.
[20] K. Takei, T. Kogai, T. Matsumoto, H. Umehara and M. Uchida, ANS Trans. 53 (1986) 219.
[21] H. Zimmermann, J. Nucl. Mater. 75 (1978) 154.
[22] K. Une and S. Kashibe, J. Nucl. Sci. Technol. 27(11) (1990) 1002.
[23] W. Miekeley and F.W. Felix, J. Nucl. Mater. 42 (1972) 297.
[24] Hj. Matzke, Radiat. Eff. 53 (1980) 219.
[25] Hj. Matzke, Radiat. Eff. 75 (1983) 317.
[26] J.C. Carter, E.J. Driscoll and T.S. Elleman, Phys. Status Solidi (a) 14 (1972) 673.
[27] J.A. Turnbull, C.A. Friskney, J.R. Findlay, F.A. Johnson and A.J. Walter, J. Nucl. Mater. 107 (1982) 168.
[28] M. Hirai, J.H. Davies and R. Williamson, J. Nucl. Mater. 226 (1995) 238.
[29] J.R. Findlay, Behaviour and Chemical State of Irradiated Ceramic Fuels, Vienna IAEA-PL-463/10 (1974) p. 211.
[30] R.M. Cornell, J. Nucl. Mater. 38 (1971) 319.
[31] C. Baker and C. Killeen, Material for Nuclear Reactor Core Application (BNES, London, 1987) Paper 24.
[32] K. Une, K. Nogita, S. Kashibe and M. Imamura, J. Nucl. Mater. 188 (1992) 65.
[33] G.L. Reynolds and B. Burton, J. Nucl. Mater. 82 (1979) 22.
[34] T. Kogai, R. Iwasaki and M. Hirai, J. Nucl. Sci. Technol. 26(8) (1989) 744.
[35] C. Vitanza, E. Kolstad and U. Graziani, ANS Topical Meeting on Light Water Reactor Fuel Performance, Portland, Oregon, April 29 to May 3, 1979.